Progress in Organic Coatings 131 (2019) 378–388

Contents lists available at ScienceDirect

Progress in Organic Coatings

journal homepage: www.elsevier.com/locate/porgcoat

Long term stability of biodegradable polymers on building limestone

Zişan Kaplan[a,*], Hasan Böke[a], Aysun Sofuoglu[b,c], Başak İpekoğlu[a]

[a] Department of Architectural Restoration, Izmir Institute of Technology, Urla, 35430, Izmir, Turkey
[b] Department of Chemical Engineering, Izmir Institute of Technology, Urla, 35430, Izmir, Turkey
[c] Environmental Research Center, Izmir Institute of Technology, Urla, 35430, Izmir, Turkey

ARTICLE INFO

Keywords:
Limestone
Biodegradable polymer
Protection
Accelerated weathering
Stability

ABSTRACT

Synthetic polymers can be replaced by biodegradable ones as adhesives, water repellents and consolidants on the stone surfaces and facades of the historic buildings in their conservation to minimize future deterioration. In this study, the long-term stability of two biodegradable polymers, polyhydroxybutyrate (PHB) and poly-L-lactide (PLA), and an acrylic polymer (Paraloid B72) which is commonly used in conservation works of artefacts, were evaluated on limestone using a UV lamp-weathering chamber (up to 104 days) for future protection studies. Chemical and morphological changes induced by an accelerated weathering test were examined by Fourier Transform Infrared spectroscopy (FT-IR) and Scanning Electron Microscopy (SEM) analyses. Protection efficiency of the polymers was determined by the changes in color, capillary water absorption, static contact angle on limestone. Paraloid B72, PHB, and PLA coatings significantly increased hydrophobicity while decreasing capillarity water absorption and caused negligible change in the color of the limestone. Protection efficiencies of PLA and PHB polymers were almost the same as that of Paraloid B72, a widely used acrylic polymer. However, PLA and PHB seemed to be favorable polymers as protective agents due to their reversibility and biodegradability, low chromatic changes, good hydrophobic behavior and good stability to weathering in reducing the effects of outdoor exposure on limestone surfaces.

1. Introduction

Natural and synthetic polymers have been used as water repellent and consolidant in the conservation of movable and built cultural heritages. The polymers used in conservation work should be reversible, re-treatable, compatible, water repellent and breathable to allow the passage of water vapor, not cause any color variation on the object, easy in application and resistant against weathering. Acrylic polymers extensively used in stone conservation to preserve monuments from further deterioration mostly fulfill these principles except reversibility [1,2].

Paraloid B72, an acrylic polymer, is widely used as adhesive, water repellent and consolidant in the conservation work of several movable or immovable artefacts [3–5]. It acts as a waterproof coating, but loses its efficiency and removability in time due to polymer decomposition [3]. The surface discoloration resulting from Paraloid B72 coating is not acceptable for the conservation of cultural heritage [3,6,7]. On the other hand, Paraloid B72 increases the water repellency (hydrophobicity) of stone surfaces while hydrophobicity decreases due to the weathering effects.

Paraloid B72 penetrates into the pores of stones producing a uniform surface and, due to outdoor conditions, it is subjected to weathering through UV light exposure, which causes degradation by chain scissions, photoinduced crystallization and cross linking [7–19]. UV irradiation leads to color changes and loss of surface hydrophobicity depending on the relative intensity of the radiation [3,7].

Biodegradable polymers, which are produced from natural resources in the natural environment during the growth cycles of organisms, that can be classified as agro-polymers and bio polyesters are used in pharmaceutics, tissue engineering and food packaging industry [20,21]. The resistance of biodegradable polymers to accelerated weathering was evaluated by previous studies [22–27]. The results of these studies indicated that, the main degradations were chains scissions and cross-linking reactions. Their average molecular weight was decreased, ester linkages were hydrolyzed, and the degree of crystallinity was increased.

The effect of certain biodegradable polymers mostly zein, chitosan, PHB and PLA as protective agents on stone surfaces were investigated in a few studies [28–34]. Zein is a thermoplastic protein with a hydrophobic nature, excellent film-forming properties and higher strength and lower gas permeability than other biopolymer films [28,32]. Chitosan is produced from chitin found in the exoskeleton of

* Corresponding author.
E-mail address: zisankaplan@iyte.edu.tr (Z. Kaplan).

https://doi.org/10.1016/j.porgcoat.2019.03.004
Received 5 November 2018; Received in revised form 22 January 2019; Accepted 3 March 2019
Available online 13 March 2019
0300-9440/

invertebrates and arthropods. PHB and PLA are bio polyesters with relatively good water barrier properties. Both of them have crystalline structures and high melting points [35,36].

The studies showed that biodegradable polymers form a thin film and exhibit negligible color variation, increased hydrophobicity and reduction in the effects of gases present in polluted air (such as SO_2) on stone surfaces [28,37,38]. However, UV light degrades the polymers and leads to reduced protection efficiency depending on light intensity, humidity and temperature. Among the biodegradable polymers investigated in the studies, PLA exhibits higher photo-stability and water protection efficiency and lower color variations [30,33,39], while PHB causes negligible color changes with good water protection efficiency on stone surfaces [34]. However, protection efficiency drastically decreases and weathering leads to loss of hydrophobicity [33,39].

Biodegradable polymers have started to be considered as alternative protective agents for the conservation of movable and built cultural heritages in the past decade. PLA and PHB are renewable, re-treatable and removable polymers. These properties are considerably significant for the sustainability of authenticity in cultural heritage conservation. Although they are high-priced materials, price is of secondary importance for the conservation of cultural heritage. In addition, their long-term stability has not been examined in detail, therefore this study is conducted to evaluate the long-term stability of biodegradable polymers. This study aimed to investigate the use of PLA and PHB as alternative surface coating agents to acrylic ones on limestone surfaces. The stabilities of PLA, PHB and Paraloid B72 on limestone were evaluated together under same conditions by accelerated weathering tests with the combination of UV light, heat and moisture. Protection efficiency of the coatings was evaluated by the changes in color, capillary water absorption, and static contact angle on limestone surfaces.

2. Experimental

2.1. Materials and sample preparation

In this study, the protection efficiency of biodegradable polymer coatings was investigated on limestone samples. Limestone is a sedimentary rock and has been the major source of architectural and statuary stone [40]. The chosen limestone was less dense (2.2 g/cm^3) and a porous stone (11.3%). Limestone was mainly composed of $CaCO_3$ and has traces of quartz, alumina, magnesium and iron oxides. It contains high amounts of amorphous silica from diatoms [41]. The samples were prepared by cutting limestone pieces into rectangular plates 1.5 cm × 2.5 cm using a Buehler Isometry cutting instrument and polished with 400-grit silicon carbide powder. The samples were then cleaned ultrasonically in deionized water and dried at 60 °C.

The biodegradable polymers were poly(L-lactide) PURASORB PL 65 (PLA) (Corbion, Netherlands) and Polyhydroxybutyrate (PHB) (Good Fellow) and the synthetic polymer was Paraloid B72 (ZAG Kimya). Based on the recent studies of the protection efficiencies of biodegradable polymers on calcareous stones under the effect of acidic deposition [28], PLA and PHB possessing higher molecular weight were chosen for their better protection performances. They are semi crystalline and have good water barrier properties. Both have the density around 1.2 (g cm^{-3}). In addition, PHB has high melting point (175–180 °C) and is a water insoluble biodegradable polymer similar to petroleum based synthetic polymers. PLA is also biodegradable, thermoplastic, aliphatic polyester derived from renewable resources. The properties of PLA are determined by the molecular architecture and the molecular weight while the melting temperature is in the range of 130–180 °C. Polymer solutions were prepared without any purification as 5% (weight/volume). The PLA solution was prepared by dissolving PLA in chloroform with magnetic stirring at room temperature for 4 h. The PHB solution was prepared by dissolving PHB in chloroform at 60°-70 °C by a reflux system for approximately 2–3 h. The Paraloid B72 solution was prepared by dissolving Paraloid B72 in acetone with magnetic stirring at room temperature for approximately 1–2 h.

Each polymer solution was applied onto a limestone plate by a dip-coating apparatus (Nima dipper) at room temperature with a 100 mm/min immersion rate and 150 mm/min retraction rate. After coating, the samples were left in an oven to volatilize the solvent at 40 °C for several hours until they reached a constant weight. The film thicknesses of biodegradable polymers (PHB and PLA) and synthetic polymer (Paraloid B72) determined by SEM analysis were approximately 30 µm and 50 µm, respectively. The four coated parallel samples were weathered in an accelerated weathering chamber and used in evaluating the protection performances of coatings.

The effects of accelerated weathering conditions on the chemical properties of the polymers were determined by FT-IR analysis on thin polymer films. Thin films were prepared by casting each polymer from solution. The polymer solutions were poured into petri dishes and left under a hood for 24 h to volatilize the solvent. The formed films were then left under vacuum at 60 °C for 24 h.

2.2. Accelerated weathering test

Accelerated weathering tests were carried out in the test chamber (QUV/se Q Lab chamber) equipped with 4 UVA-340 lamps (wavelength from 365 nm to 295 nm) at up to 80 °C temperature and 100% relative humidity.

The weathering conditions were determined in accordance with the European Standard titled “Plastics - Methods of exposure to laboratory light sources - Part 3: Fluorescent UV lamps” [42]. The samples were exposed to 8 h of UV irradiance of 0.76 (W/m^2) at 60 °C followed by 4 h of condensation without irradiation at 50 °C up to 2500 h (104 days). Almost 500 h of irritation under UV exposure may correspond to 60 months of exposure to atmospheric weathering when water protection efficiency results of Paraloid B72 coated stones have been considered [16].

2.3. Evaluation of chemical and morphological changes of polymers

The chemical and morphological changes on polymer films during weathering were monitored by Fourier Transform Infrared (FT-IR) and Scanning Electron Microscope analyses (SEM).

2.3.1. Determination of chemical changes by fourier transform infrared analysis (FT-IR)

The chemical changes on the polymer films were determined by recording the FT-IR spectrum of the films at the specified time intervals of the weathering test. For the B72, 7 measurements were taken between at 0, 25, 125, 250, 500, 750 1000 h. For PLA and PHB, 10 measurements were taken at 0, 25, 125, 250, 500, 1000, 1500, 2000, 2250, 2500 h. Spectral measurements were conducted by a Spectrum BX II FT-IR spectrometer (Perkin Elmer) operated in absorbance mode and spectra were collected with the use of 4 cm^{-1} resolution in the range of 400 to 4000 cm^{-1}.

The chemical changes on the surface of the polymer films were monitored by calculating the absorption band area of each polymer during weathering. The band areas were first normalized by dividing each band value by the band value that did not change significantly (internal standard) due to the apparent randomness of the data. The C–H stretching band at 2988 cm^{-1} were chosen for Paraloid B72, PHB and PLA, respectively, as internal standard [19,43]. Calculation of the percent change of normalized peak areas was based on the average area for virgin polymer bands and the area of the weathered polymer bands (Eq. (1)) [22,44].

$$\% \text{ change in area} = 100 \times [A_v - A_w]/A_v \quad (1)$$

where A_v and A_d are the area under peak bands for virgin and weathered sample, respectively.

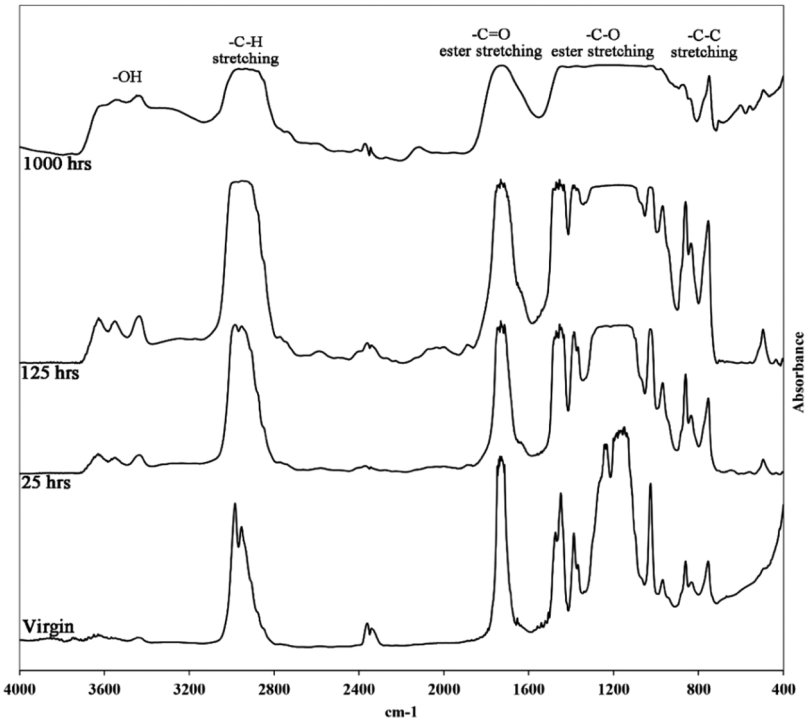

Fig. 1. FT-IR spectrum of the virgin and weathered Paraloid B72 samples.

The FT-IR results were expressed as a percentage increase or decrease in the peak area after completion of each exposure cycle. Values above zero indicate decrease in the peak areas, while values below zero indicate increase in the peak areas. A one-tailed paired sample *t*-test analysis was performed on the band areas to determine whether the final values for areas were statistically different from the original ones.

2.3.2. Determination of morphological changes by scanning Electron microscopy analysis (SEM)

Morphological changes of coated limestones were examined by Scanning Electron Microscope analysis with a FEI QUANTA 250 FEG equipped with an EDX detector (Oxford Azteck). In the analysis, samples were fixed onto aluminum stubs through carbon adhesive disks and coated with gold. Images were collected at different magnitudes by secondary electron detector at a voltage of 3 kV. Analyses were carried out at room temperature.

Removability of Paraloid B72 was tested on 2500 h weathered limestone samples by extraction with acetone. Limestone samples were treated in acetone for 24 h and acetone was evaporated. Then, SEM-EDX analysis were performed with uncoated limestone and 2500 h weathered limestone after removal of Paraloid B72 [7,16].

2.4. Evaluation of the protection performances of polymer coatings

The protection efficiency of biodegradable polymer coatings (4 parallel samples) were estimated by recording color, capillary water absorption and static contact angle of the coated and weathered samples with 9 cycles at specified time intervals between 0 and 2500 h of weathering tests.

2.4.1. Color measurements

The color change of coated and weathered samples was examined with a colorimetric measurement instrument (Avantes) by Avasoft 6.2. Measurements were conducted on the surface with 4 mm diameter spot size, D65 daylight illuminant and 10° observer. Measurements were performed at 23 ± 2 °C and 50 ± 3% relative humidity [28].

For four parallel samples, three measurements were taken on different positions of the surface of each sample. Color coordinates were determined as CIELAB (CIE L*a*b*) values. L* is the lightness (ranging from black to white), a* and b* are the chromatic coordinates (a*: green to red; b*: blue to yellow). Color differences of coated samples were calculated by the following equation (Eq. (2)). The results were expressed as ΔE^* values and uncoated limestone slabs were used as reference.

$$\Delta E = \sqrt{(\Delta L)^2 + (\Delta a)^2 + (\Delta b)^2} \quad (2)$$

2.4.2. Water absorption by capillarity measurements

The amount of water absorbed by capillarity forces were determined by measuring the amount of water that is absorbed by capillarity through the stone surface when it is in contact with water. Measurements were conducted with each coated limestone plate at 23 ± 2 °C and 50 ± 3% relative humidity before and after each period of weathering test [28]. The water protection efficiency of treated limestones was calculated as percentage change of the amount of absorbed water of coated and weathered limestones (Eq. (3)).

$$\%E \text{ (Protection Efficiency)} = (Q_i \text{ (c)} - Q_i \text{ (w)})/ Q_i \text{ (c)} *100 \quad (3)$$

where Q_i (c) is the amount of absorbed water before weathering and Q_i (w) is the amount of absorbed water after weathering.

2.4.3. Static contact angle measurements

Surface wetting properties of coated limestone samples were investigated by measuring the static contact angle of a water drop on sample surfaces with a Goniometer (Attension Theta). Measurements were conducted at 23 ± 2 °C and 50 ± 3% relative humidity.

For measurement, each polymer coated limestone plate was dried to a constant weight in an oven at 40 °C and then kept in a desiccator until the temperature reached 23 °C A micro-pipette filled with deionized water was used to deposit the drop on the sample surface slowly. The measurement was carried out after the deposition of the drop [28]. Six measurements were taken on each sample for four parallel samples to ensure reliable values.

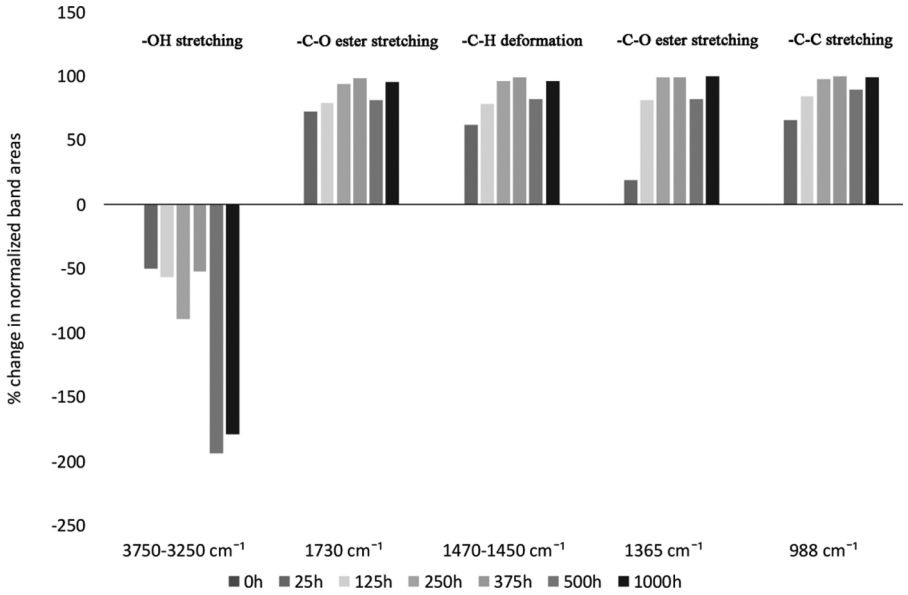

Fig. 2. % changes in the absorption band areas of the Paraloid B72 peaks after the normalization to –C–H stretching at 2988 cm^{-1} during accelerated weathering tests.

3. Results and discussion

3.1. Chemical changes on the polymer surface

The chemical changes on the polymer films were observed at the surface and deeper into the interior after weathering. The changes in Paraloid B72, PHB and PLA thin films during weathering were monitored by Fourier transform-infrared (FT-IR) spectroscopy (Figs. 1 , 3 and 5). Variations observed due to chemical changes on the normalized absorption band areas of FT-IR spectra of each polymer were presented in (Figs. 2, 4 and 6). Chemical changes in the polymers occured in a similar pattern, which is presented in the following sections.

3.1.1. Paraloid B72

The FT-IR spectrum of virgin Paraloid B72 showed the characteristic bands of C–H stretching at 2982 cm^{-1}, −C═O ester carbonyl stretching at 1730 cm^{-1}, −C−H deformation at 1475-1450 cm^{-1}, −C−O− ester stretching at 1365-1024 cm^{-1} and −C−C stretching at around 860 cm^{-1} (Fig. 1) [3,45].

FT-IR analysis showed that the degradation of Paraloid B72 started just after 25 h and gradually increased until 1000 h (Figs. 1 and 2). Statistical analysis confirmed that the mean peak area for 25 h-aged Paraloid B72 was found to be significantly lower (5% statistical significance level) compared to the mean peak area of virgin Paraloid B72 (Table 1).

The variations observed due to chemical changes at the absorption

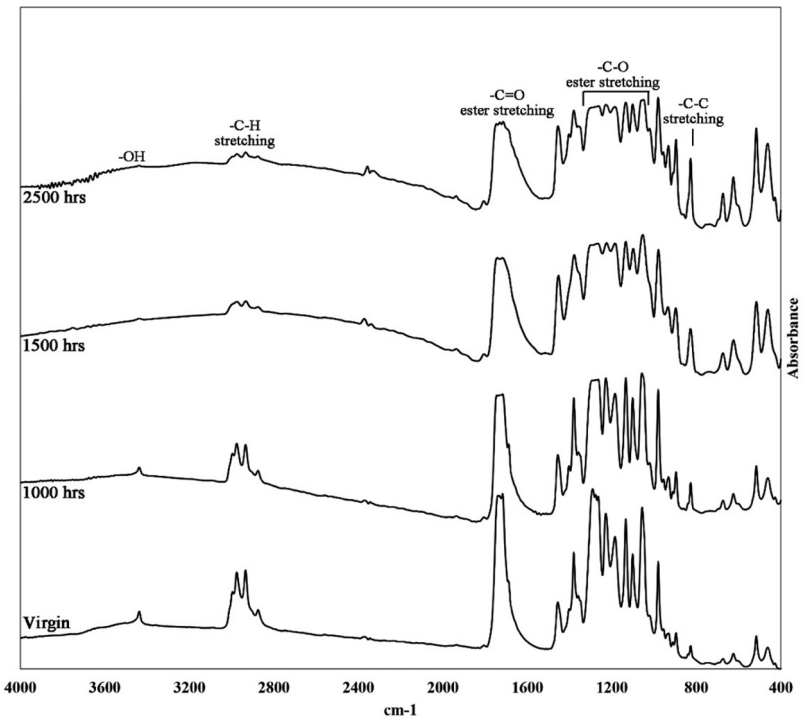

Fig. 3. FT-IR spectrum of the virgin and weathered PHB samples.

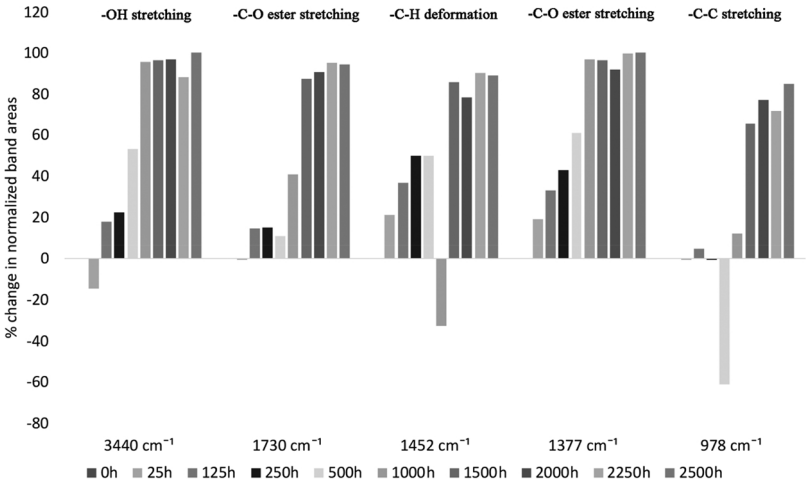

Fig. 4. % changes in the absorption band areas of the PHB peaks after the normalization to –C–H stretching at 2988 cm^{-1}, during accelerated weathering tests.

bands after 25 h weathering can be explained as follows:

i A broadening and a decrease at the absorption band of carbonyl at around 1730 cm^{-1} (-C = O ester) mainly due to the hydrolysis of ester linkages, may be causing a decrease in average molecular weight and breaking down of long macromolecular chains (Fig. 2) [8,19].
ii Formation of a weak band at 1645 cm^{-1} (C═C) due to the formation of small fragments by chain scissions, causing the polymer to acquire a yellowish hue [14,24,25,46].
iii An increase at the absorption band 3750 and 3250 cm^{-1} related to hydroxyl groups (−OH), due to the formation of carboxylic acid and hydroperoxides, resulting in the loss of hydrophobicity of the polymer (Fig. 2) [14,45].

3.1.2. Polyhydroxybutyrate (PHB)

Similarly, the FT-IR spectrum of virgin PHB showed the characteristic bands of −OH stretching at 3430 cm^{-1}, −C−H stretching at 2973 cm^{-1}, −C═O ester stretching at 1730 cm^{-1}, C−H deformation at 1450–1350 cm^{-1}, C−O− stretching ester at 1277–1054 cm^{-1} and −C−C− stretching at 978 cm^{-1} (Fig. 3) [22,44]. The chemical changes observed at the absorption bands of PHB after 1000 h could be explained as follows:

FT-IR analysis results indicated that the chemical changes of PHB started at 1000 h of weathering and then gradually increased with each weathering cycle (Figs. 3 and 4). One-tailed paired sample *t*-test analysis confirmed the statistical significance of the difference between the mean peak areas at 0 and 1000 h of weathering (Table 1).

The changes seen in the absorption bands after 1000 h of weathering could be explained as follows;

i A broadening and a decrease at the absorption band of carbonyl at around 1730 cm^{-1} (-C = O ester) mainly due to the hydrolysis of ester linkages, may be causing a decrease in average molecular

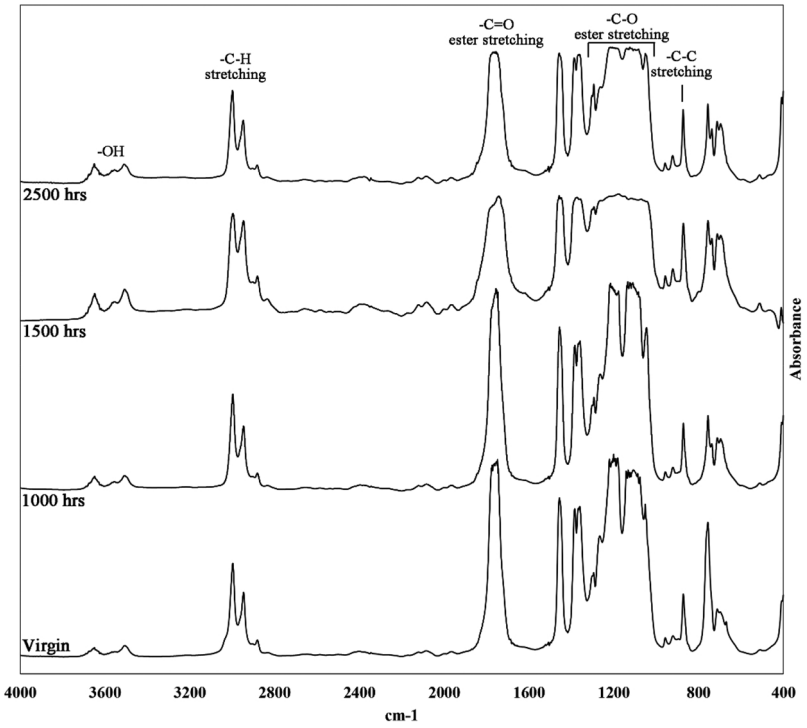

Fig. 5. FT-IR spectrum of the virgin and weathered PLA samples.

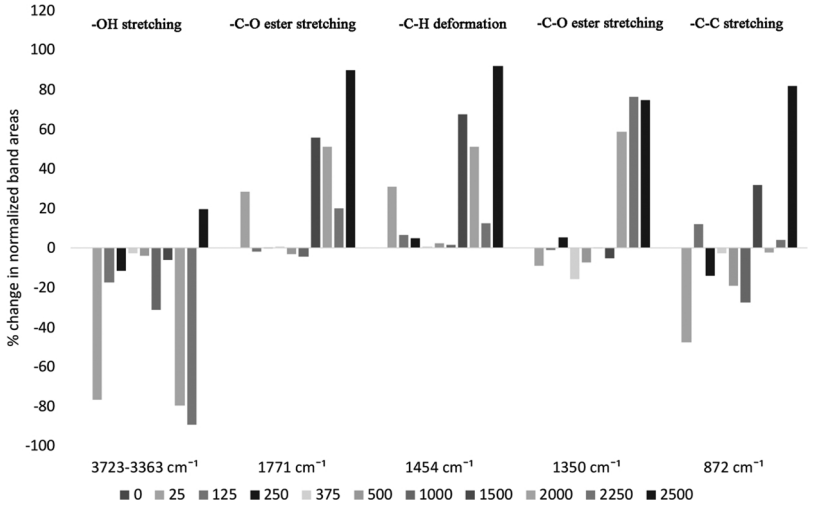

Fig. 6. % changes in the absorption band areas of the PLA peaks after the normalization to –C–H stretching at 2988 cm^{-1} during accelerated weathering tests.

Table 1
Results of the one-tailed paired sample Welch approximation *t*-test with peak mean areas of polymer spectra of virgin and weathered samples.

	Paraloid B72		PHB		PLA	
	Virgin	25 hrs	Virgin	1000 hrs	Virgin	1000 hrs
Peak Mean (% change)	180.2	49	78.7	22.1	89.7	92.2
***t*-test (P Value)**		0.07**		0.06**		0.39***
Null Hypothesis	1000 h and 0 h peak values are identical		2500 h and 0 h peak values are identical		2500 h and 0 h peak values are identical	
Result	Reject the null hypothesis: 1000 h values are significantly lower		Reject the null hypothesis: 2500 h values are significantly lower		Reject the null hypothesis: 2500 h values are significantly lower	

*denotes significance at 10%, **5%, ***.1%.

weight and breaking down of long macromolecular chains (Fig. 4) [43,47].

ii A weak band formed at 1845 cm^{-1} (C═O–) due to acetic anhydride formation, causing decreased strength [24,25,46].

iii An increase in –C–C stretching at 978 cm^{-1} due to the change in the degree of crystallinity of the polymer, leading to an increase in density, stiffness and strength [24,43].

iv An increase in the CO_2 region at 2200 cm^{-1} due to UV irradiation, causing degradation of the polymer [26].

v A decrease in the –OH region at 3525-3390 cm^{-1} related to thermal decomposition of tertiary hydroperoxides (Fig. 4) [3,22,38,45,48].

3.1.3. Poly-L-Lactide (PLA)

The FT-IR spectrum of virgin PLA showed the characteristic bands of –OH stretching at 3723-3636 cm^{-1}, –C–H stretching at 2988 cm^{-1}, –C═O ester stretching at 1771 cm^{-1}, –CH– deformation at 1450–1350 cm^{-1}, –C–O– ester stretching at 1277-1055 cm^{-1} and –C–C– stretching at 872 cm^{-1} (Fig. 5) [24,49].

The chemical changes of PLA started at 1000 h and then gradually increased with each weathering cycle (Figs. 5 and 6). This was confirmed by statistical analysis (Table 1). Since the mean peak areas for 1000 h-aged PLA were found to be significantly lower (1% statistical significance level) than the mean peak areas of virgin PLA.

The changes identified in the absorption bands after 1000 h weathering could be explained as follows;

i A broadening and a decrease at the absorption band of carbonyl at around 1730 cm^{-1} (-C = O ester) due to the hydrolysis of ester linkages, may be causing a decrease in average molecular weight and breaking down of long macromolecular chains (Fig. 6) [24,43,47].

ii An increase at the –C–C stretch band at 872 cm^{-1} due to the change in the degree of crystallinity of the polymer by increased temperature, improving physical characteristics of the polymer (60°) (Fig. 6) [24,43].

iii An increase in the CO_2 region at 2200 cm^{-1} due to UV irradiation, causing degradation of the polymer [26].

iv A weak band formed at 1845 cm^{-1} (C═O–) due to acetic anhydride formation by UV irradiation, causing etching on the polymer surfaces [24,25,46].

v An increase in the –OH region at 3700-3360 cm^{-1} due to the formation of carboxylic acid and hydroperoxides, which resulted in the loss of hydrophobicity of the polymer [22,24,25,38,43,48].

The chemical changes on all of the polymer films can be summarized by hydrolysis of ester linkages, change in the degree of crystallinity, increase in the CO_2, formation of carboxylic acid, formation of acetic anhydride and hydroperoxides. All these chemical changes resulting in a decrease at the average molecular weight and a breaking down of long macro molecular chains, as well as etching, loss of hydrophobicity, increase in density stiffness and strength and changes in color (cause yellowing) on the polymer surfaces.

3.2. Morphological changes of polymer

The structural characteristics of the limestone, the surface morphology of the polymers and the influence of weathering on polymer surfaces were investigated by SEM.

The uncoated limestone samples exhibited a slightly rough surface with the presence of small and large grains-sized calcite crystals and with diatoms distributed randomly through the stone (Fig. 7). The polymer coatings on the limestone surfaces were smooth and uniformly spread. Paraloid B72 produced a uniform flat surface with 8–10 μm layer thickness on the limestone (Fig. 7a). PHB produced a coralloid surface with 10–15 μm layer thickness and with pores of mostly smaller than 2 μm (Fig. 7c). The PLA coating had a surface with 10–15 μm layer thickness and very fine pores approximately 8 μm in size, which were regularly distributed and interconnected with each other (Fig. 7e).

All polymer coatings showed signs of chemical changes that caused surface damages. Etching, holes, voids and growth of calcite crystals in the pores were observed on the PHB-coated surfaces (Fig. 7d).

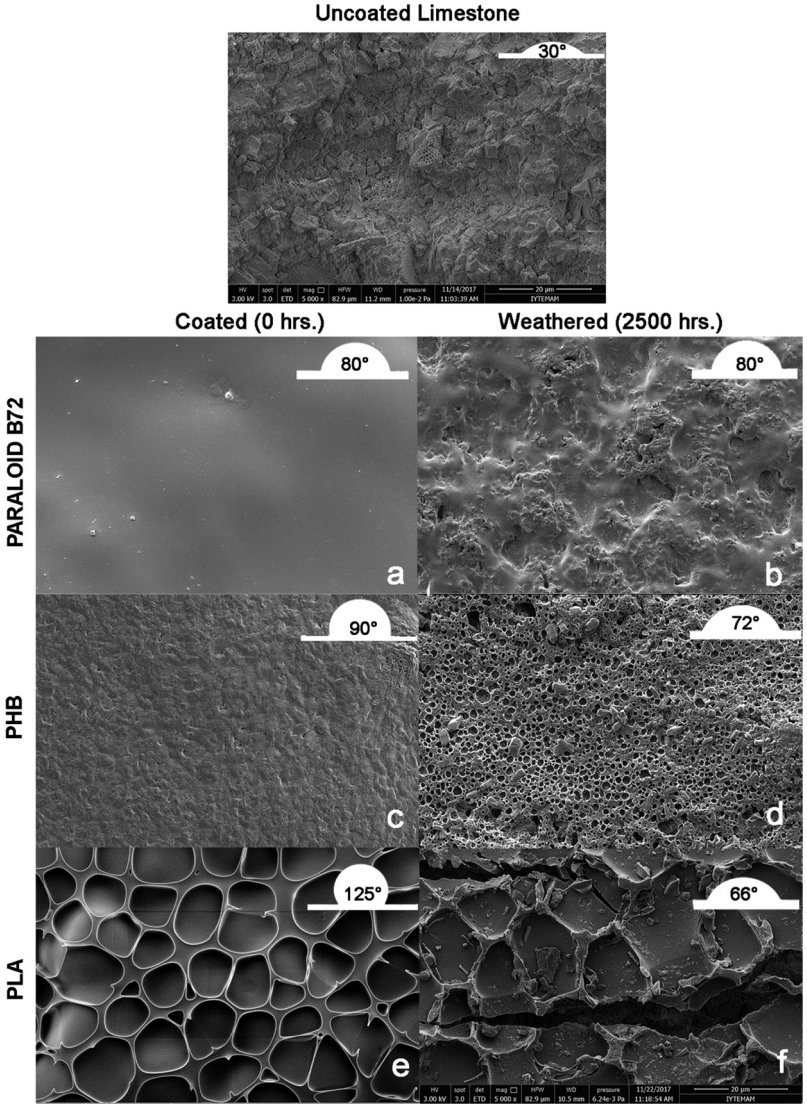

Fig. 7. SEM images (x5000) of the coated (0 h.) and weathered (2500 h.) limestone samples.

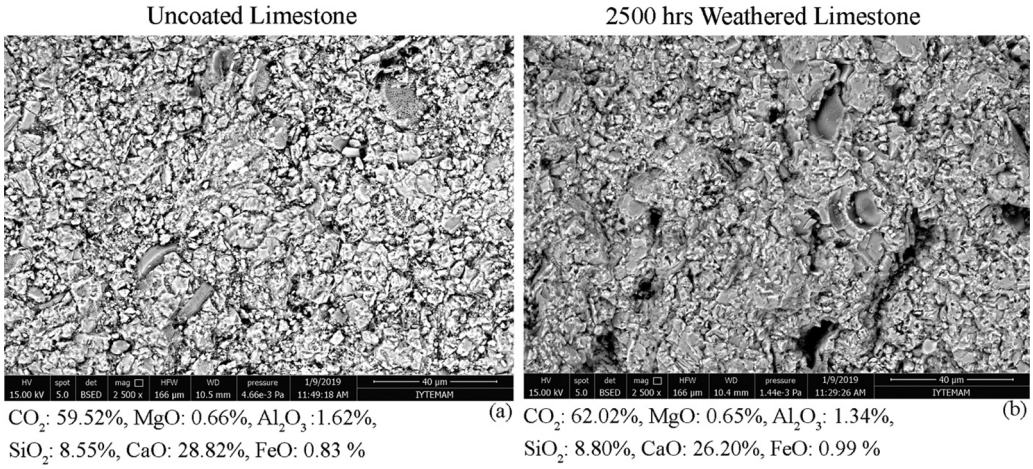

CO_2: 59.52%, MgO: 0.66%, Al_2O_3 :1.62%, SiO_2: 8.55%, CaO: 28.82%, FeO: 0.83 %

CO_2: 62.02%, MgO: 0.65%, Al_2O_3: 1.34%, SiO_2: 8.80%, CaO: 26.20%, FeO: 0.99 %

Fig. 8. SEM images of uncoated (a) and Paraloid B 72 removed limestone (b) surfaces and their % oxide compositions.

Detachment of the polymer film from surface, etching, irregular crazes and cracks, holes and voids were indicated on the PLA-coated limestone (Fig. 7f). These damages could have originated from chain scission, breaking of polymer bonds and formation of volatile gaseous products during the weathering of PLA and PHB. Solubility reduction of Paraloid B72 is investigated by removing the films on stone surface with acetone and by calculating the % differences of CO_2 and CaO contents of uncoated and Paraloid B72 removed limestone surfaces through SEM-EDX

Table 2
L*, a*, b* values and errors of coated and weathered limestone samples.

		Limestone	coated	250 hrs	500 hrs	1000 hrs	1500 hrs	1750 hrs	2000 hrs	2250 hrs
L*	Paraloid B72	62.5 ± 0.8	54.8 ± 1.2	56.9 ± 1.3	56.7 ± 1.9	54.6 ± 1.6	57.4 ± 2.1	57.2 ± 3.7	58.2 ± 1.0	56.6 ± 2.3
	PHB		64.4 ± 9.2	65.7 ± 6.5	67.5 ± 6.4	67.3 ± 6.8	67.6 ± 5.8	68.13 ± 5.91	68.84 ± 7.34	69.04 ± 7.10
	PLA		60.6 ± 1.9	62.8 ± 1.2	63.2 ± 0.9	63.0 ± 1.7	65.9 ± 0.4	66.55 ± 0.16	66.09 ± 0.53	64.58 ± 2.08
a*	Paraloid B72	0.4 ± 0.1	0.3 ± 0.1	−0.1 ± 0.1	0.0 ± 0.0	0.1 ± 0.1	0.3 ± 0.1	0.2 ± 0.4	0.0 ± 0.1	0.1 ± 0.3
	PHB		0.0 ± 0.3	−0.2 ± 0.1	−0.1 ± 0.0	−0.2 ± 0.1	0.4 ± 0.1	0.1 ± 0.1	−0.2 ± 0.1	−0.3 ± 0.1
	PLA		0.0 ± 0.1	0.1 ± 0.1	0.1 ± 0.0	0.1 ± 0.1	0.5 ± 0.1	0.2 ± 0.1	0.2 ± 0.1	0.1 ± 0.1
b*	Paraloid B72	5.1 ± 0.3	8.1 ± 0.9	6.1 ± 1.0	5.1 ± 1.0	5.2 ± 0.7	4.9 ± 0.5	6.13 ± 1.81	5.22 ± 0,39	6.01 ± 2.67
	PHB		4.2 ± 4.5	2.0 ± 2.3	2.0 ± 2.2	0.0 ± 2.0	0.4 ± 1.7	0.75 ± 1.77	1.09 ± 2.02	0.64 ± 1.92
	PLA		6.3 ± 0.3	3.5 ± 0.7	2.6 ± 0.9	1.8 ± 0.5	1.4 ± 0.6	1.47 ± 0.65	2.20 ± 0.59	3.87 ± 0.09

analysis. SEM-EDX analysis indicated that between 4–9 % solubility reduction of Paraloid B72 was observed possibly due to the effect of fast and extensive cross linking of the long ester groups (Fig. 8) [45].

3.3. Surface color changes

Since color stability of coated stone surfaces is an important factor used in the selection of polymers for the protection of historic stone buildings, a polymer used as coating material on stone surfaces should not significantly change surface color. The acceptable total color change (ΔE*) should be lower than 5, the standard accepted by the International Conservation Community of Historic Monuments and Buildings [50], whereas the human eye perception threshold is lower than 3 [51,52]. In this study, surface color changes of uncoated, coated and weathered polymer surfaces were indicated by L*, a*, b* values and ΔE* values (Table 2).

The lightness values (L* = black to white) of Paraloid B72 and PLA treated limestones were found to be lower than the uncoated one. However, the lightness value was found to be higher than the uncoated one for PHB coated surface. The lower L* values indicated that Paraloid B72 and PLA coated stone surfaces were slightly more darkened than uncoated surfaces. During accelerated weathering cycles, the L* value of B72 fluctuated but the trend was slightly downward. However, the L* values of PHB and PLA coated limestones increased as weathering progressed, causing whitening on limestones due to significant changes in surface roughness [39,48].

The a* (green to red) and b* (blue to yellow) values were found to be higher in Paraloid B72 and PLA but lower in PHB as compared with the uncoated ones. The b* values of all polymers slightly decreased and a* values of B72 and PLA slightly increased with weathering period. However, the a* value of PHB decreased during weathering.

The total color change (ΔE*) of Paraloid B72 treated limestones was higher than the threshold (< 5) reported by the International Conservation Community of Historic Monuments and Buildings. However, ΔE* values of the PHB and PLA treated limestones were near the threshold for human eye perception (< 3) [53]. At the end of the accelerated weathering test (2500 h.), the ΔE* values of Paraloid B72 and PHB treated limestones were higher than the acceptable total color change value for the conservation of cultural heritage, while the ΔE* value of PLA coated limestones was lower than the human eye perception threshold (Fig. 9).

Color measurements showed that PLA did not significantly change the surface color of the stone and exhibited better color stability after weathering than Paraloid B72 and PHB, since it maintained low ΔE* values.

3.4. Water protection efficiency

Water protection efficiency for coatings on limestone samples was determined using water absorption by capillarity and static contact angle measurements during weathering tests.

3.4.1. Water absorption by capillarity

Water absorption by capillarity test results showed that all the polymer treatments improved water protection efficiency by reducing the amount of absorbed water (Fig. 10, Table 3). Coatings with Paraloid B72 and PLA on limestone provided approximately 80% and 90% protection efficiency, respectively, while PHB treatment provided 40%. Paraloid B72 and PLA coated limestones fairly maintained their water protection efficiency (E%) until 500 h of weathering, after which the water protection efficiency drastically decreased. In contrast with Paraloid B72 and PLA, the amount of absorbed water remained constant in PHB treated limestone samples during weathering (Fig. 10). After 2500 h of weathering, none of the coatings retained their efficiency in preventing water penetration into the stone.

The loss of water protection efficiency of polymers can be explained by the detachment of the polymer film from the surface, as well as, the formation of etchings, irregular crazes, cracks, holes and voids on coating surfaces due to the effects of UV light, heat and moisture during weathering.

3.4.2. Contact angle measurements

The water contact angle of limestone was determined as 30°, indicating the hydrophilicity of limestone surface. Polymer treatment increased the contact angle of limestone. Paraloid B72 and PHB treatments increased the contact angle to 80° and 90°, respectively, which was a borderline case and would almost be accepted as hydrophobic (Figs. 7 and 11). The higher contact angle value was obtained on PLA coated limestones around 125°, which was above the borderline of hydrophobicity. The hydrophobicity of a surface directly related with the surface free energy (or coating material) and surface roughness (microstructure) [54]. PLA coating significantly increased the surface hydrophobicity, by increasing the surface roughness more than those of Paraloid B72 and PHB (Fig. 7).

The static contact angle of PHB and PLA treated limestones significantly decreased down to the hydrophobicity line after 1000 h of weathering (Fig. 11). On the contrary, the static contact angle of Paraloid B72 coated limestone was not significantly affected by weathering and still retained a contact angle of approximately 80°.

Hydrophobicity of a surface is directly related with the surface topography of the coating. SEM analysis showed that the coatings degraded by etching, irregular crazes, cracks, holes and voids that resulted in the reduction of surface hydrophobicity.

4. Conclusion

In this study, protection efficiency of Paraloid B72, PHB and PLA as coating agents on limestone were investigated under accelerated weathering conditions. Paraloid B72, PHB and PLA coatings significantly decreased capillary water absorption, increased hydrophobicity and caused negligible change in the color of the limestone.

All polymers deteriorated to some extent by exposure to UV light and the combination of high humidity and temperature. Paraloid B72 was decomposed by decomposition of ester groups, formation of

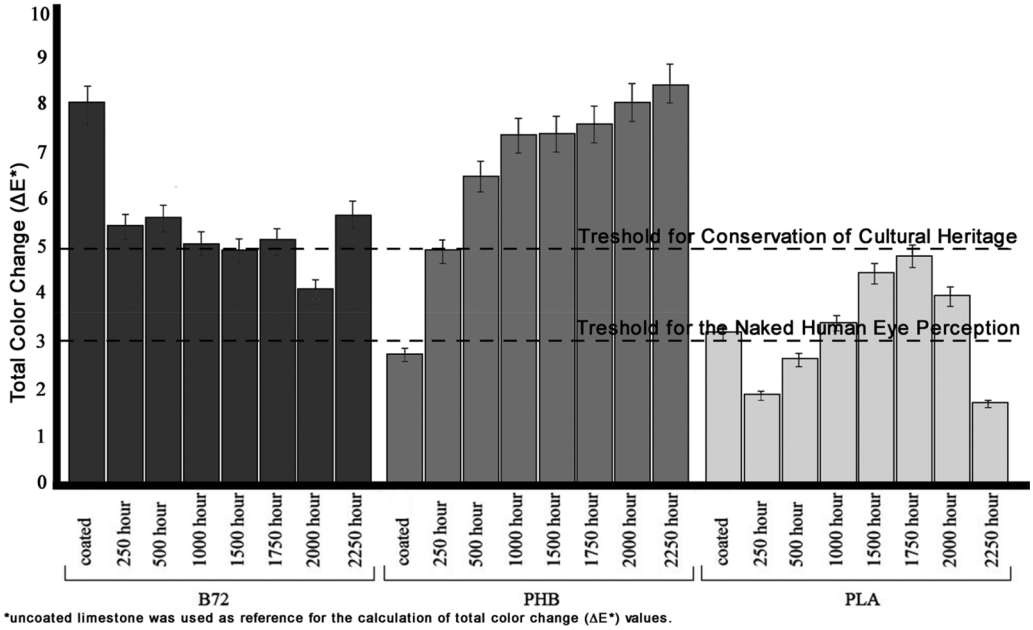

Fig. 9. Total color change values (ΔE*) of coatings during accelerated weathering tests.

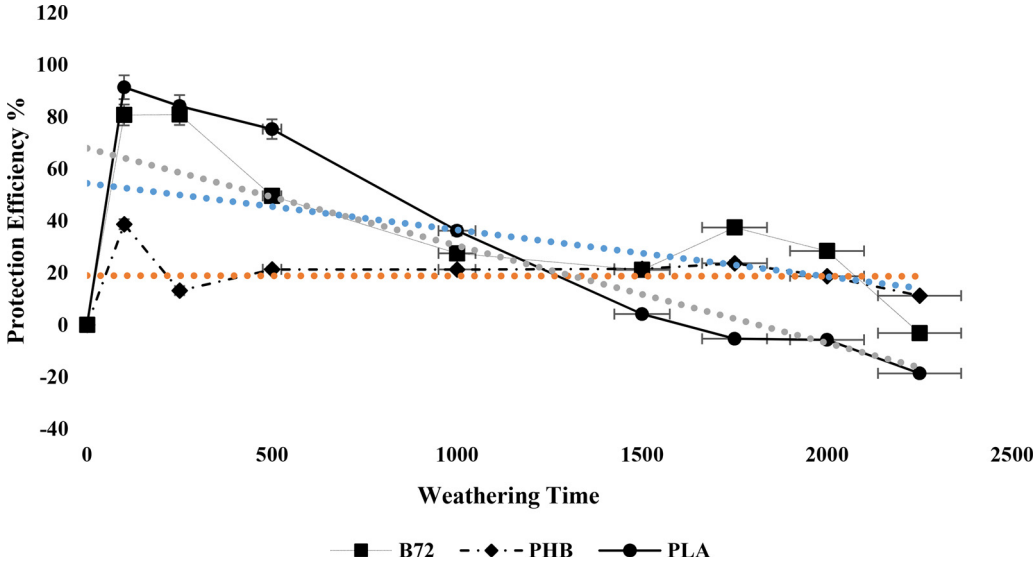

Fig. 10. Protection efficiency (%) of water absorption by capillarity of the coatings during accelerated weathering tests.

Table 3
Water absorption by capillarity values (Qi: kg/m^2) during accelerated weathering tests.

	uncoated	coated	250 hrs	500 hrs	1000 hrs	1500 hrs	1750 hrs	2000 hrs	2250 hrs
B72	0.16 ± 0.02	0.03 ± 0.01	0.03 ± 0.01	0.08 ± 0.04	0.12 ± 0.04	0.13 ± 0.03	0.10 ± 0.05	0.12 ± 0.04	0.17 ± 0.05
PHB		0.10 ± 0.03	0.14 ± 0.06	0.13 ± 0.02	0.13 ± 0.02	0.13 ± 0.01	0.12 ± 0.01	0.13 ± 0.01	0.14 ± 0.01
PLA		0.01 ± 0.00	0.03 ± 0.00	0.04 ± 0.02	0.10 ± 0.04	0.15 ± 0.02	0.17 ± 0.05	0.17 ± 0.02	0.19 ± 0.02

gamma lactones and hydroperoxides and cross linking of the ester groups. PHB and PLA were decomposed with the formation of CO_2 and hydroperoxide, hydrolysis of ester groups and reduction of the molecular weight.

All coating agents demonstrated chemical, physical and optical changes under accelerated weathering conditions. Accelerated weathering tests led to surface color change along with etching, holes, voids and cracks due to chain scission, breaking of polymer bonds and formation of volatile gaseous products.

The biodegradable polymers PLA and PHB and the widely used acrylic polymer Paraloid B72 tested in the study yielded very similar color changes and water protection efficiencies after accelerated weathering tests. However, PLA and PHB seem to be more suitable polymers as protective agents due to their reversibility and biodegradability, low chromatic changes, good hydrophobic behavior and good stability to weathering in reducing the effects of outdoor exposure on limestone surfaces.

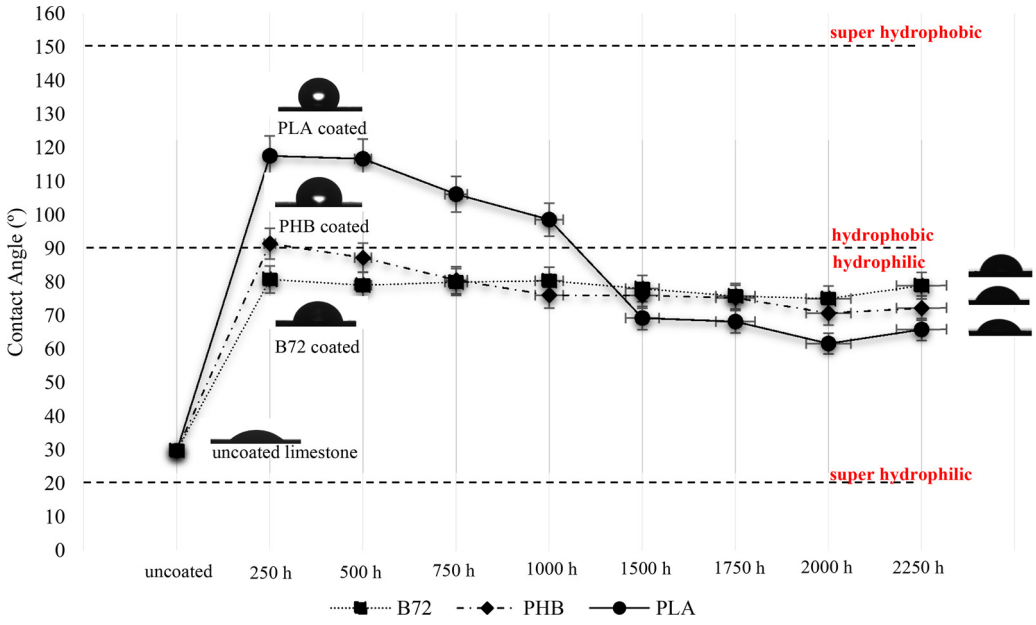

Fig. 11. Water contact angle values of uncoated, coated and coated-aged limestones.

References

[1] C.V. Horie, Material for conservation, Museum Int. 40 (1988) 120, https://doi.org/10.1111/j.1468-0033.1989.tb00742.x.

[2] ICOMOS, Icomos Charter- Principles for the Analysis, Conservation and Structural Restoration of Architectural Heritage (2003) principles, Archit. Herit (2003) 3–6.

[3] M.J. Melo, S. Bracci, M. Camaiti, O. Chiantore, F. Piacenti, Photodegradation of acrylic resins used in the conservation of stone, Polym. Degrad. Stab. 66 (1999) 23–30, https://doi.org/10.1016/S0141-3910(99)00048-8.

[4] M.F. Vaz, J. Pires, A.P. Carvalho, Effect of the impregnation treatment with Paraloid B-72 on the properties of old Portuguese ceramic tiles, J. Cult. Herit. 9 (2008) 269–276, https://doi.org/10.1016/j.culher.2008.01.003.

[5] V. Sabatini, C. Cattò, G. Cappelletti, F. Cappitelli, S. Antenucci, H. Farina, M.A. Ortenzi, S. Camazzola, G. Di Silvestro, Protective features, durability and biodegration study of acrylic and methacrylic fluorinated polymer coatings for marble protection, Prog. Org. Coat. 114 (2018) 47–57, https://doi.org/10.1016/j.porgcoat.2017.10.003.

[6] G. Alessandrini, M. Aglietto, V. Castelvetro, F. Ciardelli, R. Peruzzi, L. Toniolo, Comparative evaluation of fluorinated and unfluorinated acrylic copolymers as water-repellent coating materials for stone, J. Appl. Polym. Sci. 76 (2000) 962–977, https://doi.org/10.1002/(SICI)1097-4628(20000509)76:6<962::AID-APP24>3.0.CO;2-Z.

[7] M. Favaro, R. Mendichi, F. Ossola, U. Russo, S. Simon, P. Tomasin, P.A. Vigato, Evaluation of polymers for conservation treatments of outdoor exposed stone monuments. Part I: photo-oxidative weathering, Polym. Degrad. Stab. 91 (2006) 3083–3096, https://doi.org/10.1016/j.polymdegradstab.2006.08.012.

[8] R.A. Nyquist, W.J. Potts, Infrared absorptions characteristic of organic carbonate derivatives and related compounds, Spectrochim. Acta 17 (1961) 679–697, https://doi.org/10.1016/0371-1951(61)80135-5.

[9] E. Yousif, R. Haddad, Photodegradation and photostabilization of polymers, especially polystyrene: Review, Springerplus 2 (2013) 1–32, https://doi.org/10.1186/2193-1801-2-398.

[10] K. Wojciechowski, G.Z. Zukowska, I. Korczagin, P. Malanowski, Effect of TiO_2 on UV stability of polymeric binder films used in waterborne facade paints, Prog. Org. Coat. 85 (2015) 123–130, https://doi.org/10.1016/j.porgcoat.2015.04.002.

[11] T.V. Nguyen, X.H. Le, P.H. Dao, C. Decker, P. Nguyen-Tri, Stability of acrylic polyurethane coatings under accelerated aging tests and natural outdoor exposure: the critical role of the used photo-stabilizers, Prog. Org. Coat. 124 (2018) 137–146, https://doi.org/10.1016/j.porgcoat.2018.08.013.

[12] J.F. Rabek, Polymer Photodegradation: Mechanism and Experimental Methods, Chapman Hall, UK, 1995, https://doi.org/10.1007/978-94-011-1274-1.

[13] N.S. Allen, C.J. Regan, R. McIntyre, B.W. Johnson, W.A.E. Dunk, The photooxidation and stabilisation of water-borne acrylic emulsions, Prog. Org. Coat. (1997), https://doi.org/10.1016/S0300-9440(97)00065-9.

[14] O. Chiantore, M. Lazzari, Photo-oxidative stability of paraloid acrylic protective polymers, Polymer (Guildf). 42 (2001) 17–27, https://doi.org/10.1016/S0032-3861(00)00327-X.

[15] C. Miliani, M. Ombelli, A. Morresi, A. Romani, Spectroscopic study of acrylic resins in solid matrices, Surf. Coat. Technol. 151–152 (2002) 276–280, https://doi.org/10.1016/S0257-8972(01)01606-1.

[16] S. Bracci, M.J. Melo, Correlating natural ageing and Xenon irradiation of Paraloid?? B72 applied on stone, Polym. Degrad. Stab. 80 (2003) 533–541, https://doi.org/10.1016/S0141-3910(03)00037-5.

[17] M. Sadat-Shojai, A. Ershad-Langroudi, Polymeric coatings for protection of historic monuments: opportunities and challenges, J. Appl. Polym. Sci. 112 (2009) 2535–2551, https://doi.org/10.1002/app.29801.

[18] E. Doehne, C.A. Price, Stone Conservation: An Overview of Current Research, 2nd edition, (2010), https://doi.org/10.1016/0006-3207(70)90031-5.

[19] D. Scalarone, M. Lazzari, O. Chiantore, Acrylic protective coatings modified with titanium dioxide nanoparticles: comparative study of stability under irradiation, Polym. Degrad. Stab. 97 (2012) 2136–2142, https://doi.org/10.1016/j.polymdegradstab.2012.08.014.

[20] C. Bastioli, Handbook of Biodegradable Polymers, (2011), https://doi.org/10.1097/PRS.0b013e31822adba3.

[21] L. Avérous, E. Pollet, Environmental Silicate Nano-Biocomposites, Green Energy Technol. 50 (2012), https://doi.org/10.1007/978-1-4471-4108-2.

[22] A. Copinet, C. Bertrand, S. Govindin, V. Coma, Y. Couturier, Effects of ultraviolet light (315 nm), temperature and relative humidity on the degradation of polylactic acid plastic films, Chemosphere 55 (2004) 763–773, https://doi.org/10.1016/j.chemosphere.2003.11.038.

[23] H. Tsuji, Y. Echizen, Y. Nishimura, Photodegradation of biodegradable polyesters: a comprehensive study on poly(l-lactide) and poly(-caprolactone), Polym. Degrad. Stab. 91 (2006) 1128–1137, https://doi.org/10.1016/j.polymdegradstab.2005.07.007.

[24] D. Rasselet, A. Ruellan, A. Guinault, G. Miquelard-Garnier, C. Sollogoub, B. Fayolle, Oxidative degradation of polylactide (PLA) and its effects on physical and mechanical properties, Eur. Polym. J. 50 (2014) 109–116, https://doi.org/10.1016/j.eurpolymj.2013.10.011.

[25] E. Olewnik-Kruszkowska, I. Koter, J. Skopinska-Wisniewska, J. Richert, Degradation of polylactide composites under UV irradiation at 254 nm, J. Photochem. Photobiol. A Chem. 311 (2015) 144–153, https://doi.org/10.1016/j.jphotochem.2015.06.029.

[26] J. Lim, J. Kim, UV-photodegradation of poly(3-hydroxybutyrate-co-3-hydroxyhexanoate) (PHB-HHx), Macromol. Res. 24 (2016) 9–13, https://doi.org/10.1007/s13233-016-4004-x.

[27] H. Simmons, M. Kontopoulou, Hydrolytic degradation of branched PLA produced by reactive extrusion, Polym. Degrad. Stab. 158 (2018) 228–237, https://doi.org/10.1016/j.polymdegradstab.2018.11.006.

[28] Y. Ocak, A. Sofuoglu, F. Tihminlioglu, H. Böke, Protection of marble surfaces by using biodegradable polymers as coating agent, Prog. Org. Coat. 66 (2009) 213–220, https://doi.org/10.1016/j.porgcoat.2009.07.007.

[29] M. Frediani, L. Rosi, M. Camaiti, D. Berti, A. Mariotti, A. Comucci, C. Vannucci, I. Malesci, Polylactide/perfluoropolyether block copolymers: Potential candidates for protective and surface modifiers, Macromol. Chem. Phys. 211 (2010) 988–995, https://doi.org/10.1002/macp.201000034.

[30] G. Giuntoli, L. Rosi, M. Frediani, B. Sacchi, P. Frediani, Fluoro-functionalized PLA polymers as potential water-repellent coating materials for protection of stone, J. Appl. Polym. Sci. 125 (2012) 3125–3133, https://doi.org/10.1002/app.36469.

[31] L. Pinho, A. Pedna, Reversible Fluorinated PLA / Sio 2 Nanocomposites as Hydrophobic Coatings for Stone, 2014 (2014), pp. 199–203.

[32] Y. Ocak, A. Sofuoglu, F. Tihminlioglu, H. Böke, Sustainable bio-nano composite coatings for the protection of marble surfaces, J. Cult. Herit. 16 (2015) 299–306, https://doi.org/10.1016/j.culher.2014.07.004.

[33] A. Pedna, L. Rosi, M. Frediani, P. Frediani, High glass transition temperature polyester coatings for the protection of stones, J. Appl. Polym. Sci. 132 (2015) 1–12, https://doi.org/10.1002/app.42323.

[34] S. Andreotti, E. Franzoni, P. Fabbri, Poly(hydroxyalkanoate)s-based hydrophobic coatings for the protection of stone in cultural heritage, Mater. (Basel). 11 (2018) 165, https://doi.org/10.3390/ma11010165.
[35] R. Auras, B. Harte, S. Selke, An overview of polylactides as packaging materials, Macromol. Biosci. 4 (2004) 835–864, https://doi.org/10.1002/mabi.200400043.
[36] S. Khanna, A.K. Srivastava, Recent advances in microbial polyhydroxyalkanoates, Process Biochem. 40 (2005) 607–619, https://doi.org/10.1016/j.procbio.2004.01.053.
[37] B. Sacchi, E. Cantisani, G. Giuntoli, S. Salvini, L. Rosi, M. Frediani, P. Frediani, Biopolymers as Stone protectives, 12th Int. Congr. Deterior. Conserv. Stone Columbia Univ. New York, 2012 Bio-Polymers, 2012, pp. 1–10.
[38] A. Pedna, L. Pinho, P. Frediani, M.J. Mosquera, Obtaining SiO2-fluorinated PLA bionanocomposites with application as reversible and highly-hydrophobic coatings of buildings, Prog. Org. Coat. 90 (2016) 91–100, https://doi.org/10.1016/j.porgcoat.2015.09.024.
[39] G. Giuntoli, M. Frediani, A. Pedna, L. Rosi, P. Frediani, New perspectives for application of PLA in cultural heritage, in: Vincenzo Piemonte (Ed.), Polylactic Acid Synth. Prop. Appl. 2012, pp. 161–190.
[40] K.L. Gauri, J.K. Bandyopadhyay, Carbonate Stone: Chemical Behavior, Durability, and Conservation, Wiley, 1999.
[41] G. Toprak, Characteristics of Limes Produced From Marbles and Limestones, (2007), p. 89.
[42] ISO 4892-2, Plastics – methods of exposure to laboratory light sources – Part 2: xenon-arc lamps, Int. Organ. Stand. 3 (2013).
[43] M. Agarwal, K.W. Koelling, J.J. Chalmers, Characterization of the degradation of polylactic acid polymer in a solid substrate environment, Biotechnol. Prog. 14 (1998) 517–526, https://doi.org/10.1021/bp980015p.
[44] T. Furukawa, H. Sato, R. Murakami, J. Zhang, Y.X. Duan, I. Noda, S. Ochiai, Y. Ozaki, Structure, dispersibility, and crystallinity of poly(hydroxybutyrate)/ poly (L-lactic acid) blends studied by FT-IR microspectroscopy and differential scanning calorimetry, Macromolecules 38 (2005) 6445–6454, https://doi.org/10.1021/ma0504668.
[45] M. Lazzari, O. Chiantore, Thermal-ageing of paraloid acrylic protective polymers, Polymer (Guildf). 41 (2000) 6447–6455, https://doi.org/10.1016/S0032-3861(99)00877-0.
[46] M. Gardette, S. Thérias, J.-L. Gardette, M. Murariu, P. Dubois, Photooxidation of polylactide/calcium sulphate composites, Polym. Degrad. Stab. 96 (2011) 616–623, https://doi.org/10.1016/j.polymdegradstab.2010.12.023.
[47] L. Wei, A.G. McDonald, Accelerated weathering studies on the bioplastic, poly(3-hydroxybutyrate-co-3-hydroxyvalerate), Polym. Degrad. Stab. 126 (2016) 93–100, https://doi.org/10.1016/j.polymdegradstab.2016.01.023.
[48] R.K. Sadi, G.J.M. Fechine, N.R. Demarquette, Photodegradation of poly(3-hydroxybutyrate), Polym. Degrad. Stab. 95 (2010) 2318–2327, https://doi.org/10.1016/j.polymdegradstab.2010.09.003.
[49] E. Meaurio, N. López-Rodríguez, J.R. Sarasua, Infrared spectrum of poly(L-lacticde): application to crystallinity studies, Macromolecules 39 (2006) 9291–9301, https://doi.org/10.1021/ma061890r.
[50] J.F. Illescas, M.J. Mosquera, Producing surfactant-synthesized nanomaterials in situ on a building substrate, without volatile organic compounds, ACS Appl. Mater. Interfaces 4 (2012) 4259–4269, https://doi.org/10.1021/am300964q.
[51] R. Berns, F. Billmeyer, M. Saltzman, Principles of color technology, J. Dent. 247 (2000), https://doi.org/10.1002/col.1038.
[52] I. De Rosario, F. Elhaddad, A. Pan, R. Benavides, T. Rivas, M.J. Mosquera, Effectiveness of a novel consolidant on granite: Laboratory and in situ results, Constr. Build. Mater. 76 (2015) 140–149, https://doi.org/10.1016/j.conbuildmat.2014.11.055.
[53] I.E. Ruyter, K. Nilner, B. Möller, Color stability of dental composite resin materials for crown and bridge veneers, Dent. Mater. 3 (1987) 246–251, https://doi.org/10.1016/S0109-5641(87)80081-7.
[54] Y. Shen, J. Tao, H. Tao, S. Chen, L. Pan, T. Wang, Nanostructures in superhydrophobic Ti6Al4V hierarchical surfaces control wetting state transitions, Soft Matter 11 (2015) 3806–3811, https://doi.org/10.1039/c5sm00024f.